

# Constitutive glycogen synthase kinase-3 $\alpha$ / $\beta$ activity protects against chronic $\beta$ -adrenergic remodelling of the heart

Ian G. Webb<sup>1</sup>, Yasuhiro Nishino<sup>1</sup>, James E. Clark<sup>1</sup>, Colin Murdoch<sup>1</sup>, Simon J. Walker<sup>1</sup>, Marcus R. Makowski<sup>2</sup>, Rene M. Botnar<sup>2</sup>, Simon R. Redwood<sup>1</sup>, Ajay M. Shah<sup>1</sup>, and Michael S. Marber<sup>1\*</sup>

<sup>1</sup>Division of Cardiology, King's College London BHF Centre, The Rayne Institute, St Thomas' Hospital, Lambeth Palace Road, London SE1 7EH, UK; and <sup>2</sup>Division of Imaging Sciences, King's College London BHF Centre, The Rayne Institute, St Thomas' Hospital, London SE1 7EH, UK

Received 26 October 2009; revised 17 February 2010; accepted 19 February 2010; online publish-ahead-of-print 17 March 2010

Time for primary review: 42 days

**Aims** Glycogen synthase kinase 3 (GSK-3) signalling is implicated in the growth of the heart during development and in response to stress. However, its precise role remains unclear. We set out to characterize developmental growth and response to chronic isoproterenol (ISO) stress in knockin (KI) mice lacking the critical N-terminal serines, 21 of GSK-3 $\alpha$  and 9 of GSK-3 $\beta$  respectively, required for inactivation by upstream kinases.

**Methods and results** Between 5 and 15 weeks, KI mice grew more rapidly, but normalized heart weight and contractile performance were similar to wild-type (WT) mice. Isolated hearts of both genotypes responded comparably to acute ISO infusion with increases in heart rate and contractility. In WT mice, chronic subcutaneous ISO infusion over 14 days resulted in cardiac hypertrophy, interstitial fibrosis, and impaired contractility, accompanied by foetal gene reactivation. These effects were all significantly attenuated in KI mice. Indeed, ISO-treated KI hearts demonstrated reversible physiological remodelling traits with increased stroke volume and a preserved contractile response to acute adrenergic stimulation. Furthermore, simultaneous pharmacological inhibition of GSK-3 in KI mice treated with chronic subcutaneous ISO recapitulated the adverse remodelling phenotype seen in WT hearts.

**Conclusion** Expression of inactivation-resistant GSK-3 $\alpha$ / $\beta$  does not affect eutrophic myocardial growth but protects against pathological hypertrophy induced by chronic adrenergic stimulation, maintaining cardiac function and attenuating interstitial fibrosis. Accordingly, strategies to prevent phosphorylation of Ser-21/9, and consequent inactivation of GSK-3 $\alpha$ / $\beta$ , may enable a sustained cardiac response to chronic  $\beta$ -agonist stimulation while preventing pathological remodelling.

**Keywords** GSK-3 • Cardiac hypertrophy • Remodelling

## 1. Introduction

Glycogen synthase kinase 3 (GSK-3) is a highly conserved serine/threonine kinase implicated as a key signalling mediator in a range of cardiovascular diseases, including ischaemic myocardial conditioning,<sup>1,2</sup> myocardial hypertrophy,<sup>3,4</sup> and progressive heart failure.<sup>5,6</sup> Two isoforms, GSK-3 $\alpha$  and GSK-3 $\beta$ , are ubiquitously expressed with high sequence homology within their catalytic domains.<sup>7</sup>

Cardiac myocyte hypertrophy is a normal feature of both post-natal eutrophic growth and adaptive physiological growth.<sup>8,9</sup> Maladaptive pathological hypertrophy, however, may result from myocardial infarction, pressure overload or as a direct response to neurohormonal activation, often recapitulated experimentally using angiotensin receptor, endothelin receptor or  $\beta$ -adrenoceptor agonists. At the subcellular level, there is reactivation of foetal gene programmes, differential protein expression, and altered intracellular calcium

\* Corresponding author. Tel: +44 20 7188 1008; fax: +44 20 7188 0970, Email: mike.marber@kcl.ac.uk

Published on behalf of the European Society of Cardiology. All rights reserved. © The Author 2010. For permissions please email: journals.permissions@oxfordjournals.org. The online version of this article has been published under an open access model. Users are entitled to use, reproduce, disseminate, or display the open access version of this article for non-commercial purposes provided that the original authorship is properly and fully attributed; the Journal, Learned Society and Oxford University Press are attributed as the original place of publication with correct citation details given; if an article is subsequently reproduced or disseminated not in its entirety but only in part or as a derivative work this must be clearly indicated. For commercial re-use, please contact journals.permissions@oxfordjournals.org.

handling.<sup>10,11</sup> Ultimately, these lead to irreversible interstitial fibrosis and progressive contractile impairment.

GSK-3 has been identified in a variety of experimental models as an important signalling mediator in all forms of myocardial hypertrophy through direct inhibitory regulation of key downstream transcriptional and translational effectors.<sup>12–14</sup> Kinase activity is primarily controlled by inactivation through N-terminal phosphorylation of serine-9 of GSK-3 $\beta$  and serine-21 of GSK-3 $\alpha$ . GSK-3 $\beta$  inactivation occurs in response to pharmacological agonists (e.g. endothelin-1 and  $\alpha$ - and  $\beta$ -adrenoceptor agonists) and trans-aortic banding.<sup>4,15,16</sup> Hypertrophy in response to these interventions is significantly attenuated by overexpression of inactivation-resistant GSK-3 $\beta$  (Ser-9-Ala).<sup>3,4</sup> Likewise, co-expression of this transgene with a mutant  $\beta$ -myosin heavy chain ( $\beta$ -MHC), to mimic familial hypertrophic cardiomyopathy, reduces cardiac mass.<sup>17</sup> Furthermore, temporally regulated GSK-3 $\beta$  overexpression suggests that reactivation can regress established pressure-overload hypertrophy.<sup>18</sup>

Persistent prevention of GSK-3 $\beta$  inactivation within the heart raises potential concerns, however. Overexpression of inactivation-resistant or wild-type (WT) GSK-3 $\beta$ , for example, is associated with abnormal developmental growth,<sup>3,11</sup> while overexpression of kinase-dead 'dominant-negative' GSK-3 $\beta$  results in basal ventricular hypertrophy but significantly reduces fibrosis, apoptosis, and cardiac dysfunction in response to pressure overload.<sup>6</sup> Further uncertainty is introduced through manipulation of the equally abundant GSK-3 $\alpha$  isoform, where activation appears to reduce heart size but promote fibrosis, apoptosis, and heart failure after aortic banding.<sup>19</sup>

Although the heterogeneity in current data may, in part, reflect the diversity in timing and isoform-specificity of GSK-3 targeting, additional concerns have been highlighted in the common experimental use of transgene overexpression.<sup>20</sup> More recently, a novel genetic mouse model of endogenous GSK-3 allele targeting has been described, in which the regulatory N-terminal serine residues are selectively mutated to non-phosphorylatable alanine, rendering both GSK-3 isoforms constitutively active.<sup>21</sup> Prior characterization of this line suggests normal developmental growth and response in adult hearts to pressure overload.<sup>22</sup> We set out to examine the response in this mouse model to an alternative pro-hypertrophic stress, and to further clarify any baseline and stress-induced cardiovascular responses associated with constitutive GSK-3 activity.

## 2. Methods

Further Methods are available in the Supplementary material online. All experiments performed conform with the Guide for the Care and Use of Laboratory Animals published by the US National Institutes of Health (NIH Publication No. 85-23, revised 1996) and in accordance with United Kingdom Home Office Guidance on the Operation of Animals (Scientific Procedures) Act 1986, published by Her Majesty's Stationary Office, London.

### 2.1 GSK-3 $\alpha/\beta$ double-knockin mice

The targeting strategy and consequent effect on the PKB/Akt-GSK3-GS signalling axis have been described before.<sup>21,23</sup> Further experiments were performed in this study using isolated murine hearts perfused with isoproterenol (ISO) to confirm activation of PKB/Akt and characterize downstream signalling in WT and knockin (KI) mice.

### 2.2 GSK-3 signalling and acute haemodynamic response to adrenergic stimulation

Adult male mice (25–30 g) were anaesthetized with intraperitoneal pentobarbital (300 mg/kg) and heparin (150 U). Hearts were rapidly isolated

and perfused in Langendorff-mode, as described previously.<sup>23</sup> A fluid-filled balloon within the left ventricular (LV) cavity monitored contractile function and ventricular rate. After 30 min stabilization, the perfusate was then switched every 10 min to a 10-fold greater concentration of ISO (Sigma, I5627; Krebs–Henseleit buffer as a solvent, concentration range  $10^{-10}$ – $10^{-6}$  mol). Additional experiments were performed with  $10^{-8}$  mol ISO (approximate log EC<sub>50</sub>) or control buffer only, perfused for 15 min after stabilization and hearts snap-frozen in liquid nitrogen for protein analysis.

### 2.3 Chronic exposure to ISO and (2'Z, 3'E)-6-bromoindirubin-3'-oxime

Subcutaneous 14-day osmotic pumps (Alzet, Durect; model 1002) containing ISO (Sigma, I5627; 30 mg/kg/day) or vehicle (0.9% NaCl) were inserted into adult mice (25–30 g males) under 2% isoflurane/oxygen anaesthesia. To determine whether pharmacological inhibition of GSK-3 activity would rescue myocardial sensitivity to ISO infusion in KI mice, we used daily intraperitoneal delivery of (2'Z, 3'E)-6-bromoindirubin-3'-oxime (300  $\mu$ L of 50 nMol solution; Calbiochem, 361550), or BIO, previously shown to achieve sustained systemic kinase inhibition *in vivo*.<sup>24</sup> KI mice treated with BIO received daily intraperitoneal injections for 14 days [300  $\mu$ L of a 50 nMol BIO solution prepared in DMSO:NaCl (0.9%), 1:10]. Confirmation of GSK-3 inhibition with this protocol in our mice was determined through interrogation of the GSK-3 endogenous substrate, glycogen synthase. Briefly, hearts from WT and KI mice, subjected to intraperitoneal injection of BIO (300  $\mu$ L of 50 nMol BIO), were rapidly extracted at 4, 12, and 24 h and snap-frozen in liquid nitrogen for immunoblotting and quantification of total and phosphorylated protein.

At 14 days, invasive LV pressure analysis and echocardiography were performed. Hearts were excised for immunoblotting, histology, and RT-PCR. Later experiments involved removal of pumps at Day 14, recovery for an additional 14 days, and repeat echocardiography to assess cardiac structure and function.

### 2.4 Morphometric analysis

Hearts arrested in diastole (300  $\mu$ L of 15% KCl intracardiac) were mounted on a Langendorff-rig surrounded by 10% paraformaldehyde (PFA). LV chamber pressure was maintained at 10 mmHg and a further 10 mL of 10% PFA retrogradely perfused via the aorta. After 10 min, the balloon was removed and hearts stored in 10% PFA at 4°C for 24 h. Hearts were then placed in 2.5% glutaraldehyde for 1 min and set in 5% agarose. Seven hundred-micrometre thick sections were image-scanned for off-line analysis (Adobe Photoshop 7.0). Serial measurements were taken at the level of the mid-papillary muscle.

### 2.5 Immunoblotting

Immunoblotting experiments set out to determine (i) the phosphorylation status of GSK-3 $\alpha/\beta$ , (ii) kinase activity through endogenous substrate phosphorylation, and (iii) the integrity of the PKB/Akt-GSK-3 signalling pathway in response to ISO stimulation. Full experimental materials are included in the Supplementary material online.

### 2.6 Histology

Paraffin-mounted LV sections (8  $\mu$ m) from the level of the mid-papillary muscle were stained with picosirius red (0.1% w/v), isolectin-B4 (Vector B-1205; 1:200), or wheat germ agglutinin–rhodamine (Vector RL-1022; 1:50). Apoptosis was determined by terminal deoxynucleotidyl transferase-mediated dUTP nick end-labelling (TUNEL) (Roche). Cardiac fibrosis was calculated from picosirius red-stained sections viewed under circular polarized light, according to a modified Junqueira method.<sup>25,26</sup> Myocyte area (by planimetry), capillary density, and TUNEL-positive nuclei were measured from images obtained by confocal microscopy using digital analysis software (SigmaScan Pro 5.0).

## 2.7 Real-time RT–PCR

Total RNA was purified from LV homogenate using an SV RNA extraction kit (Promega, UK). Atrial natriuretic factor (ANF),  $\alpha$ -skeletal actin (ASA), and  $\beta$ -actin mRNA expression was analysed by real-time RT–PCR using fluorescent SYBR Green technology on a Prism 7000 HT system (Applied Biosystems, USA). Standard curves were constructed from cDNA standards for ANF and ASA, and results normalized by expression as a molar/molar ratio to  $\beta$ -actin. Details of primers are available in the Supplementary material online.

## 2.8 Echocardiography

Serial echocardiography (Visualsonic Vevo 770™, 30 MHz linear signal transducer) was performed under isoflurane/oxygen anaesthesia before pump implantation (Day 0), at Days 14 and 28. Averaged M-mode measures from parasternal long-axis images were recorded. Interventricular septal and LV posterior wall (LVPW) dimensions were taken in diastole and systole, in addition to LV internal dimensions (LVIDd and LVIDs, respectively). Fractional shortening (FS) was calculated as  $(LVIDd - LVIDs/LVIDd) \times 100$  and ejection fraction as  $(LVIDd^3 - LVIDs^3)/LVIDd^3 \times 100$ .

Further interrogation of *in vivo* cardiac contractile performance by magnetic resonance imaging (MRI) and invasive haemodynamic measurements appear in the Supplementary material online.

## 2.9 Statistical analyses

Data are presented as means  $\pm$  SEM. Comparisons between groups were assessed for significance by analysis of variance (ANOVA), repeated measures ANOVA, or analysis of covariance (ANCOVA), as appropriate. When significant differences were detected, individual mean values were compared by Bonferroni's *post hoc* test. *P*-values  $< 0.05$  were considered significant.

## 3. Results

### 3.1 Characterization of GSK-3 $\alpha/\beta$ inactivation-resistant mice

GSK-3 $\alpha/\beta$  KI mice were phenotypically comparable to WT animals from the same colony. As previously reported, KI mice were heavier over the 5–15 week age range evaluated (Figure 1A).<sup>21</sup> However, normalized heart weight (HW) did not differ significantly by genotype. Myocardial content of PKB/Akt, GSK-3, and glycogen synthase protein was also comparable, consistent with existing data (Figure 1B).<sup>21,23</sup> Specifically,  $\alpha$ - and  $\beta$ -isoforms were present in approximately equal abundance and unchanged by targeting. In isolated WT hearts, acute ISO exposure resulted in significant GSK-3 $\beta$

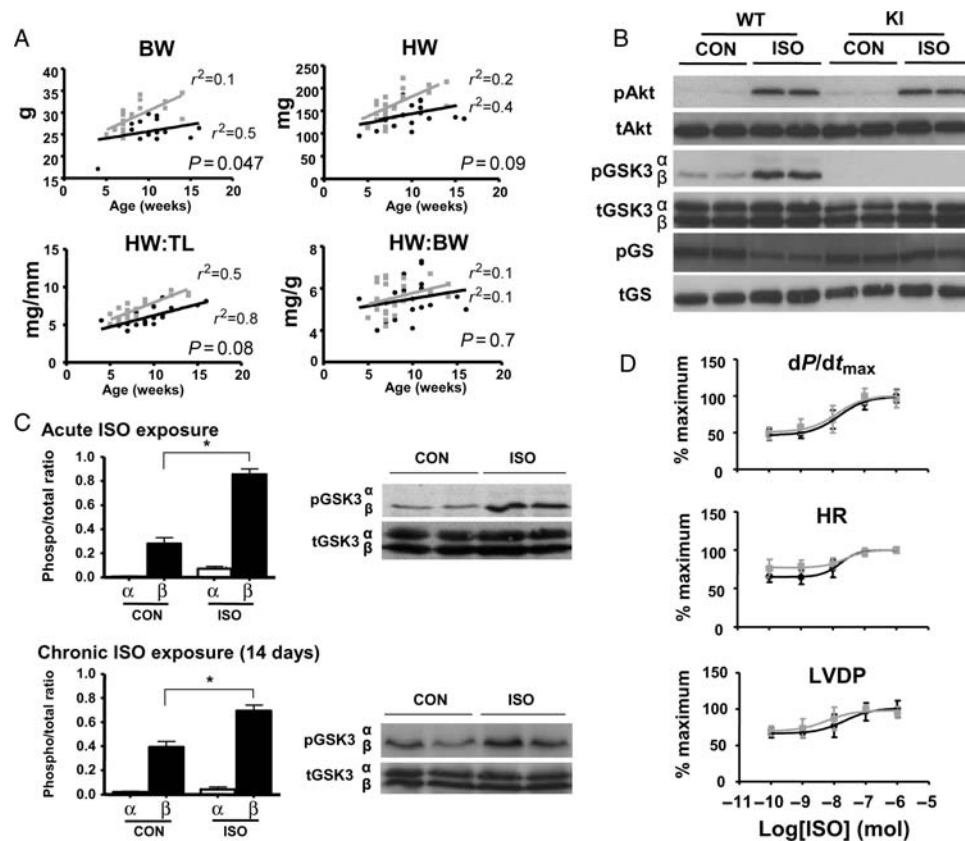


**Figure 1** Developmental growth and baseline characteristics of WT (GSK-3 $\alpha/\beta$ <sup>Ser-21/9</sup>) and KI (GSK-3 $\alpha/\beta$ <sup>Ala-21/9</sup>) mice. (A) Heart weight (HW), body weight (BW), and tibia length (TL) measurements in a cohort of male mice between 5 and 15 weeks of age.  $n = 25$  (grey square, KI) and  $n = 20$  (black circle, WT). (B) Representative western blots of isolated hearts perfused for 15 min with ISO ( $10^{-8}$  mol) or control (Krebs–Henseleit buffer). (C) GSK-3 $\alpha/\beta$  phosphorylation profile in response to acute and chronic ISO exposure. Representative immunoblots are shown with quantitative analyses of repeat experiments expressed as the ratio of phosphorylated to total protein. Data expressed as mean  $\pm$  SEM ( $n = 4$ ), \* $P < 0.05$  vs. control. (D) Concentration–response relationship for isolated hearts perfused with ISO;  $dP/dt_{max}$ , contractile performance; HR, heart rate; LVDP, left ventricular developed pressure. Black circle, WT; grey square, KI,  $n = 6$ /group, NS between genotypes in all categories.

(Ser-9), but not GSK-3 $\alpha$  (Ser-21), phosphorylation (Figure 1B and C). Kinase activity in KI hearts was inferred through examination of downstream glycogen synthase, which is basally phosphorylated as a result of constitutive GSK-3 activity and this was unchanged by acute ISO treatment (Figure 1B). A similar GSK-3 phosphorylation profile was demonstrated after 14 days treatment with chronic subcutaneous ISO (Figure 1C).

Baseline haemodynamic measurements in isolated-perfused hearts (Figure 1D) and *in vivo* from pressure-volume interrogation (data not shown) were equivalent between genotypes. Similarly, dose-response profiles to acute ISO stimulation did not differ (Figure 1D). Specifically, peak, trough, and log EC<sub>50</sub> measures of heart rate, LV developed pressure (LVDP), and systolic contractile performance (dP/dt) were all comparable between genotypes (see Supplementary material online, Table S1).

### 3.2 Effects of chronic ISO exposure on GSK-3 $\alpha$ / $\beta$ inactivation-resistant hearts

Chronic ISO treatment over 14 days caused a significant increase in normalized HW in WT animals vs. within-genotype control [HW/body weight (BW)  $6.7 \pm 0.2$  vs.  $5.4 \pm 0.1$ , HW/tibia length (TL)  $9.1 \pm 0.3$  vs.  $7.2 \pm 0.1$ , respectively,  $n \geq 10$ ,  $P < 0.05$ ] (Figure 2A), consistent with increases in mean LV and septal wall thickness measured from mounted sections at the level of the mid-papillary muscle ( $1.9 \pm 0.04$  vs.  $1.3 \pm 0.09$  and  $1.5 \pm 0.07$  vs.  $1.1 \pm 0.06$  mm, respectively,  $n = 6$ ,  $P < 0.05$ ) (Figure 2D and Table 1). Baseline HW/BW and HW/TL ratios in age-matched KI mice tended to be higher than WT, consistent with earlier phenotype characterization, but did not differ significantly. KI hearts, however, were resistant to

ISO-driven hypertrophy with marked attenuation of the morphological changes seen in WT counterparts, such as HW/BW and HW/TL ratios ( $6.2 \pm 0.3$  vs.  $6.0 \pm 0.2$  and  $8.4 \pm 0.4$  vs.  $8.3 \pm 0.2$ , respectively,  $n \geq 10$ , NS) (Figure 2A), as well as mean LV and septal morphometry in ISO and vehicle control ( $1.4 \pm 0.04$  vs.  $1.6 \pm 0.08$  and  $1.3 \pm 0.07$  vs.  $1.2 \pm 0.05$  mm, respectively,  $n = 6$ , NS) (Table 1). Invasive measures of aortic pressure at 2 weeks treatment failed to detect any significant differences between the genotypes or between ISO and vehicle exposure (data not shown).

We then set out to determine whether pharmacological inhibition of GSK-3 activity would rescue myocardial sensitivity to ISO treatment in KI mice (Figure 2B). Initial examination of pGSK-3 and p-glycogen synthase levels in hearts of both genotypes at 4 h after intraperitoneal injection of BIO (300  $\mu$ L of 50 nMol BIO) was able to confirm reduction in glycogen synthase phosphorylation levels, independent of GSK-3 phosphorylation status (Figure 2C). Sampling of glycogen synthase and other endogenous substrates at 12 and 24 h, however, gave inconclusive results, possibly due to cycling and heterogeneity of upstream phosphorylating effectors and/or phosphatases.

We proceeded to daily intraperitoneal administration of BIO (300  $\mu$ L of 50 nMol) in KI mice treated with 14-day subcutaneous ISO or vehicle; this latter group was considered more appropriate than the WT controls in which GSK-3 activity is already inhibited by ISO and a hypertrophic phenotype manifest. As demonstrated in Figure 2A, BIO co-administration with ISO was able to restore hypertrophy in KI hearts compared with vehicle controls receiving BIO alone (HW/BW:  $7.3 \pm 0.2$  vs.  $5.4 \pm 0.2$ ; HW/TL:  $10.1 \pm 0.2$  vs.  $7.3 \pm 0.4$ , respectively,  $n = 10$ ,  $P < 0.05$ ), with proportional changes in mean LV wall thickness on cross-sectional morphology (mean LV

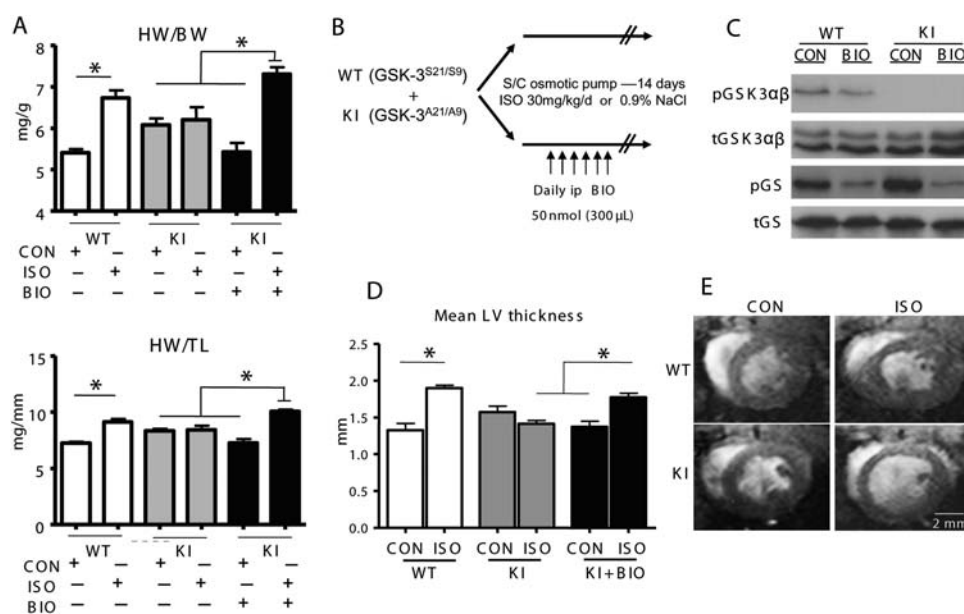


**Figure 2** Response to chronic exposure to ISO or vehicle control and/or BIO. (A) Heart weight/body weight (HW/BW) and heart weight/tibia length (HW/TL) in mice exposed to 14-day ISO, vehicle control (CON), and/or intraperitoneal BIO;  $n \geq 10$ /group,  $*P < 0.05$ . (B) Protocol for pharmacological GSK-3 inhibition; KI mice subjected to chronic 14-day exposure with ISO/CON additionally received daily intraperitoneal injections of BIO (300  $\mu$ L of 50 nmol). (C) Representative western blots from hearts snap-frozen at 4 h after intraperitoneal BIO injection. (D) Morphological measurements of mean LV wall thickness recorded from 700  $\mu$ m-thick sections at the mid-papillary level in hearts;  $n = 6$ /group,  $*P < 0.05$ . (E) Representative cross-sectional MR images of hearts at end-diastole at 14-day treatment. Images were acquired under isoflurane anaesthesia and are taken at the level of the mid-papillary muscle.

**Table 1** Heart morphology data

	GSK-3 WT		GSK-3 KI		GSK-3 KI + BIO	
	CON	ISO	CON	ISO	CON	ISO
HW/BW (mg/g)	5.4 ± 0.1	6.7 ± 0.2*	6.0 ± 0.2	6.2 ± 0.3	5.4 ± 0.2	7.3 ± 0.2 <sup>††</sup>
LV thickness (mm)	1.3 ± 0.09	1.9 ± 0.04*	1.6 ± 0.08	1.4 ± 0.04 <sup>#</sup>	1.4 ± 0.08	1.8 ± 0.05 <sup>††</sup>
Septal thickness (mm)	1.1 ± 0.06	1.5 ± 0.07*	1.2 ± 0.05	1.3 ± 0.07	1.1 ± 0.05	1.3 ± 0.07
LV septal thickness (mm)	0.2 ± 0.03	0.4 ± 0.06	0.4 ± 0.06	0.2 ± 0.05	0.3 ± 0.09	0.5 ± 0.09 <sup>†</sup>
LV:septal ratio	1.2 ± 0.03	1.3 ± 0.05	1.4 ± 0.04	1.0 ± 0.15	1.3 ± 0.08	1.4 ± 0.08 <sup>†</sup>
RV free wall thickness (mm)	0.5 ± 0.06	0.6 ± 0.03	0.6 ± 0.03	0.5 ± 0.03	0.5 ± 0.04	0.6 ± 0.05

After 14-day treatment with ISO or vehicle control, hearts were arrested in diastole (15% KCl), excised, and fixed in 10% paraformaldehyde with an intra-ventricular pressure of 10 mmHg. Mean left ventricular wall and septal thickness measurements were recorded from 700 µm-thick sections at the level of the mid-papillary muscle.  $n = 6$ /group.

\* $P < 0.05$  vs. CON (within genotype).

<sup>†</sup> $P < 0.05$  vs. KI ISO.

<sup>††</sup> $P < 0.05$  vs. KI ISO and KI CON + BIO.

<sup>#</sup> $P < 0.05$  vs. WT ISO.

1.8 ± 0.05 vs. 1.4 ± 0.08 mm, respectively,  $n = 6$ ,  $P < 0.05$ ) (Figure 2D and Table 1). Importantly, however, GSK-3 inhibition alone in the adult KI heart had no effect in the absence of adrenergic stimulation; specifically, normalized HW measures and mean LV dimensions in this group were comparable to KI hearts subjected to ISO, or control without BIO, co-administration.

### 3.3 Fibrosis, apoptosis, and markers of cellular hypertrophy with chronic ISO

We then examined whether the gross morphological changes in response to stress were mirrored at the cellular level. Picosirius red staining was used to measure myocardial fibrosis, and confocal immunofluorescence microscopy to measure myocyte cross-sectional area, capillary density, and TUNEL-positive apoptotic nuclei. We additionally interrogated mRNA transcripts for evidence of foetal gene reactivation. WT hearts demonstrated a significant increase in myocyte cross-sectional area (Figure 3B) in response to ISO vs. control (628 ± 78.8 vs. 395.8 ± 33.6 µm<sup>2</sup>,  $n = 5$ ,  $P < 0.05$ , respectively), accompanied by fibrosis, determined both by histology and the up-regulation of genes encoding procollagen Iα1, IIIα1, and fibronectin (Figure 4A). Hypertrophied hearts also demonstrated increased TUNEL-positive nuclei (Figure 3D). Additionally, ISO induced up-regulation in genes encoding ASA and ANF (1.05 ± 0.23 vs. 0.25 ± 0.04% and 11.3 ± 2.4 vs. 5.2 ± 1.4%, respectively;  $n = 8$ ,  $P < 0.05$  within each group) (Figure 4A), as well as an increase in capillary density compared with control (9.4 ± 1.1 vs. 6.0 ± 0.7 µm<sup>-2</sup>,  $n = 5$ ,  $P < 0.05$ ) (Figure 3C). All changes in these measures were significantly attenuated in KI hearts in response to ISO, confirming resistance to pathological hypertrophic changes.

### 3.4 Physiological assessment of chronic ISO treatment and interval recovery

Serial echocardiography was performed before (baseline) and after treatment with ISO/vehicle control (Day 14). A final scan was performed 2 weeks after pump extraction (Day 28) to examine the potential for 'reverse remodelling' after removal of the stress stimulus. No baseline differences in cardiac structure or function from non-invasive assessment were evident between genotypes (Figure 5 and Table 2). In response to ISO treatment, WT hearts demonstrated significant

increases in diastolic septal and LVPW thickness at Day 14 compared with baseline (1.6 ± 0.2 vs. 1.0 ± 0.1 and 1.4 ± 0.2 vs. 0.9 ± 0.1 mm, respectively,  $n = 6$ ,  $P < 0.05$ ) (Figure 5 and Table 2). This was associated with ventricular dilatation (4.1 ± 0.5 vs. 3.4 ± 0.2 and 3.2 ± 0.3 vs. 1.5 ± 0.3 mm, respectively, for LVIDd and LVIDs,  $n = 6$ ,  $P < 0.05$ ) and impairment of cardiac function (FS: 23 ± 2 vs. 48 ± 4%,  $n = 6$ ,  $P < 0.05$ ). At Day 28, there was apparent regression of hypertrophy and a significant, but not fully reversible, reduction in internal LV dimensions. Likewise, FS demonstrated some improvement but remained significantly impaired (Table 2). Conversely, ISO-treated KI hearts maintained contractile function at Days 14 and 28, but did demonstrate reversible increases in internal LV dimensions in response to ISO (LVIDd: 3.5 ± 0.4, 4.4 ± 0.6\*, and 3.6 ± 0.2 mm; LVIDs: 1.9 ± 0.5, 2.7 ± 0.6\*, and 1.6 ± 0.2 mm, respectively, for Days 0, 14, and 28;  $n = 6$ , \* $P < 0.05$  vs. baseline), consistent with adaptive remodelling.

Similar findings were demonstrated in parallel, non-serial cardiac MRI experiments (see Supplementary material online, Table S2). Specifically, there was reversible dilatation of ISO-treated KI hearts, with attenuation of contractile impairment compared with within-genotype control. Indeed, indexed cardiac output and stroke volume significantly increased in response to 2-week ISO treatment in this genotype (713 ± 61 vs. 458 ± 38 µL/min g and 1.4 ± 0.1 vs. 0.9 ± 0.1 µL/g, respectively, vs. KI CON,  $n = 6$ ,  $P < 0.05$ ), consistent with a sustained adrenergic response in these hearts. To explore this further, we repeated experiments to interrogate interval ISO dose–response profiles in isolated-perfused hearts at the end of 14-day chronic adrenergic stimulation (Day 14) and 14 days after subcutaneous pump removal (Day 28) (Figure 6A). At Day 14, ISO-treated WT hearts demonstrated a significant reduction in adrenergic sensitivity, with blunting of dose–response profiles for LVDP and +dP/dt, compared with within-genotype controls (Figure 6B). Conversely, there was no significant difference in dose–response profiles for KI hearts compared with baseline. At Day 28, adrenergic sensitivity appeared intact in isolated KI hearts (Figure 6B), whereas there was a sustained and significant impairment in treated WT hearts following cessation of ISO.

## 4. Discussion

Our results indicate that expression of inactivation-resistant GSK-3α/β isoforms does not interfere with eutrophic myocardial growth or

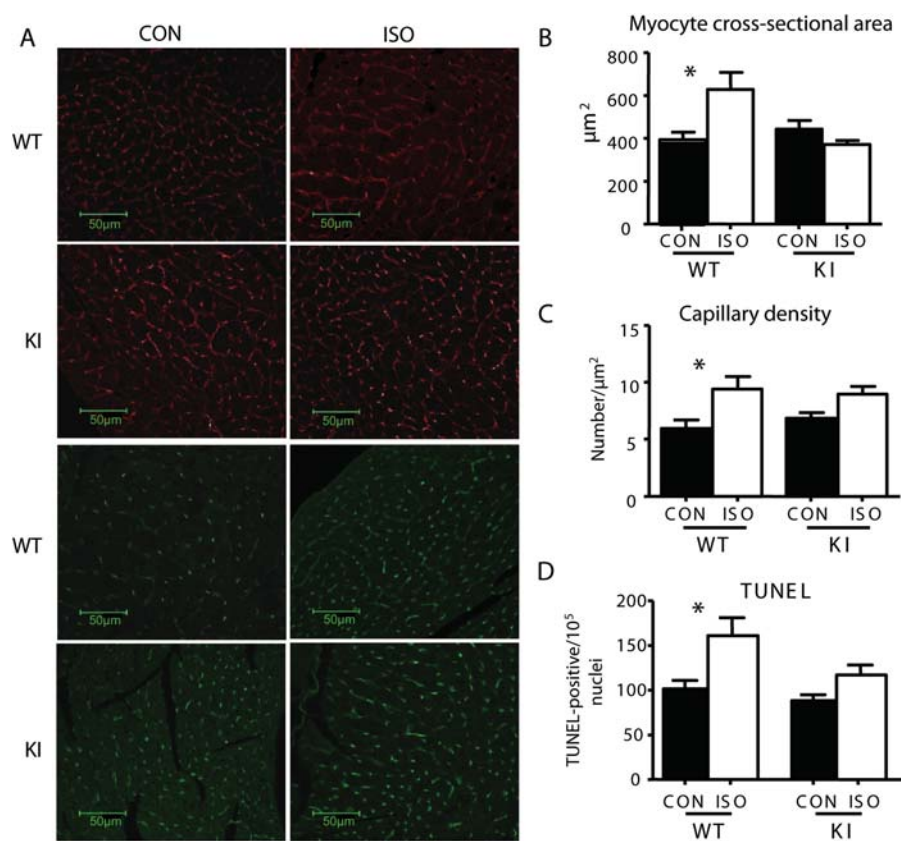


**Figure 3** Myocyte cross-sectional area, capillary density, and TUNEL staining. Representative images (A) and quantitative analysis of (B) myocyte cross-sectional area (red; wheat germ agglutinin–rhodamine), (C) capillary density (green; isolectin B4), and (D) TUNEL-positive nuclei;  $n = 5$ /group, \* $P < 0.05$ .

baseline cardiac function, but does avert the pathological hypertrophy caused by chronic ISO stress. Specifically, the increases in myocardial mass, interstitial fibrosis, and foetal gene expression in hearts of WT mice are absent in those of KI mice. Indeed, KI hearts demonstrate a paradoxical increase in indexed stroke volume and cardiac output at 2 weeks of treatment on MR imaging, a finding reversed on removal of ISO stress. Furthermore, unlike WT animals, adrenergic sensitivity and reserve are maintained in KI hearts treated with ISO, consistent with a sustained permissive physiological response to adrenergic stimulation.

N-terminal phosphorylation and consequent inactivation of GSK-3 is considered a strategic point of convergence for myocardial hypertrophy under a variety of circumstances.<sup>27</sup> Particular attention has focused on GSK-3 $\beta$  as the predominant isoform mediating these effects, with interventions that maintain GSK-3 in the active state attenuating adverse remodelling.<sup>3,4</sup> In particular, two independent laboratories have both employed cardiac-specific expression of haemagglutinin-tagged GSK-3 $\beta^{\text{ala9}}$  under the control of an  $\alpha$ -myosin heavy chain ( $\alpha$ -MHC) promoter.<sup>3,11</sup> The resultant tagged protein expression, however, vastly exceeds endogenous levels with corresponding increases in kinase activity. Furthermore, the effects on the expression of equally abundant GSK-3 $\alpha$  are unknown. This is relevant since overexpression of  $\alpha$ -MHC-driven WT GSK-3 $\alpha$  is associated with reduced cardiac growth, protection against trans-aortic banding, but a paradoxical increase in apoptosis and fibrosis.<sup>19</sup> However, it remains uncertain whether these changes truly reflect

the function of GSK-3 $\alpha$  since there is an accompanying reciprocal down-regulation of GSK-3 $\beta$ , highlighting the complexity of manipulating this signalling pathway by transgenic overexpression of individual isoforms. Additionally, although baseline  $\alpha$ -MHC promoter activity is normally high in adult mice, suppression and isogene switching to  $\beta$ -MHC are reported in experimental hypertrophy and cardiac failure.<sup>10,28</sup> Finally, transgene-driven overexpression in mouse hearts is known to induce an unfolded protein response which can reverse the expected phenotype.<sup>29</sup>

More recently, data have emerged in a novel mouse line expressing inactivation-resistant GSK-3 $\alpha$ - and  $\beta$ -isoforms, achieved through site specific mutation of the N-terminal phosphorylation serine residues to non-phosphorylatable alanine.<sup>21,22</sup> Target protein expression is comparable between KI and WT animals. In response to pressure overload induced by aortic constriction, KI mice demonstrated significant attenuation in hypertrophy, interstitial fibrosis, and cardiac dysfunction, a phenotype largely attributable to  $\beta$ -isoform manipulation. Conversely, GSK-3 $\alpha$  KI mice demonstrated an exaggerated response to pressure overload with significant hypertrophy and cardiac dysfunction. Additionally, there was attenuation of myocyte proliferation during stress.<sup>22</sup>

We set out to interrogate the response in dual isoform KI animals to an alternative hypertrophic stress and later to clarify the nature of 'positive' or 'adaptive' remodelling apparent from our early results. We specifically addressed dual isoform manipulation given the high structural homology between kinase domains and common

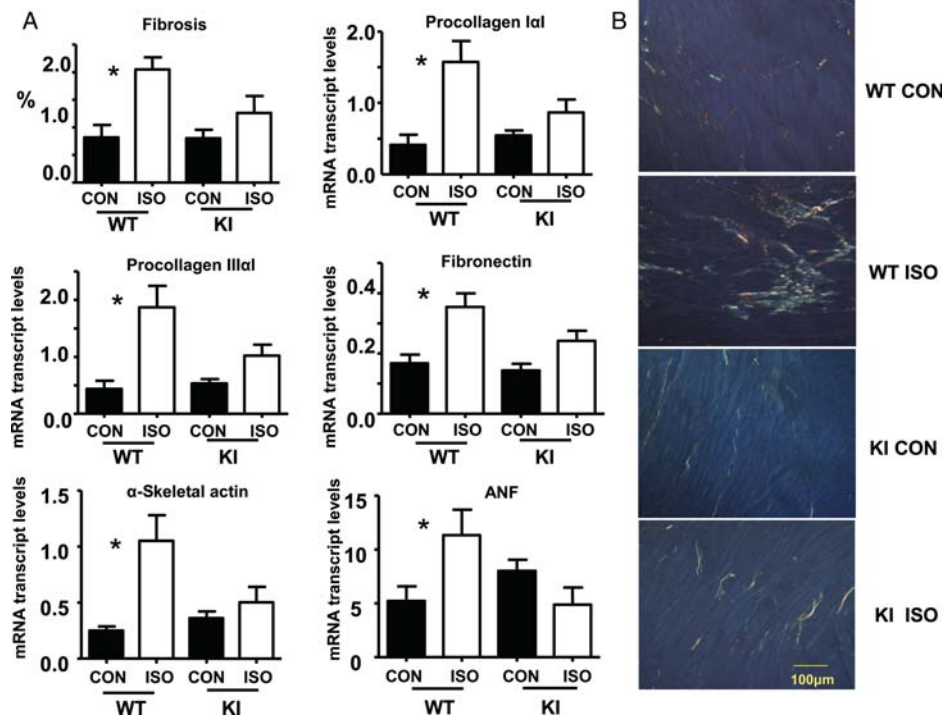


**Figure 4** Fibrosis and foetal gene reactivation. (A) Quantification of fibrosis and mRNA transcript abundance for procollagens I $\alpha$ 1, III $\alpha$ 1, and fibronectin;  $n = 5/\text{group}$ ,  $*P < 0.05$ . Additional quantification of the foetal genes, ASA and ANF, was also preformed;  $n = 8/\text{group}$ ,  $*P < 0.05$ . All transcript results are normalized to  $\beta$ -actin mRNA levels. (B) Representative examples of picosirius red-stained LV sections (8  $\mu\text{m}$  thick) viewed under circular polarized light demonstrating the effect of ISO on cardiac fibrosis.

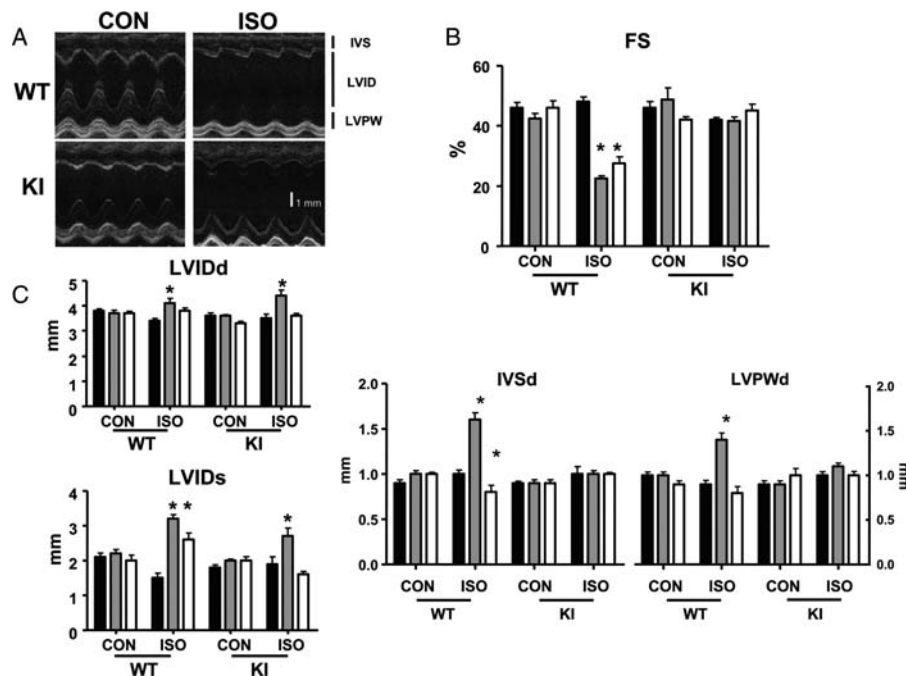


**Figure 5** Echocardiographic measures of hearts subjected to ISO or vehicle control (CON). Serial studies were performed under isoflurane inhalational anaesthesia at baseline (Day 0, black bar), after 2-week treatment (Day 14, grey bar), and after 2-week recovery (Day 28, white bar);  $n = 6/\text{group}$ ,  $*P < 0.05$  vs. within-group baseline measurements. (A) Representative long-axis parasternal echocardiographic images, IVS, interventricular septum; LVID, left ventricular internal dimension; LVPW, left ventricular posterior wall. (B) FS [= (LVIDd - LVIDs/LVIDd)  $\times$  100] and (C) Structural heart measurements taken at the mid-papillary level; LVIDd/s represent end-diastole and end-systole LVID measurements, respectively.

Table 2 Cardiac echocardiography

Time (days)	GSK-3 WT						GSK-3 KI					
	CON			ISO			CON			ISO		
	0	14	28	0	14	28	0	14	28	0	14	28
HR (b.p.m.)	453 ± 14	464 ± 35	406 ± 14	475 ± 26	412 ± 31*	397 ± 30*	425 ± 52	485 ± 39*	436 ± 12	450 ± 40	469 ± 80	422 ± 32
EF (%)	78 ± 5	74 ± 5	78 ± 7	80 ± 4	46 ± 4*	54 ± 9*	78 ± 5	76 ± 3	74 ± 3	74 ± 2	72 ± 4	77 ± 5
FS (%)	46 ± 5	43 ± 5	46 ± 6	48 ± 4	23 ± 2*	28 ± 6*	46 ± 5	49 ± 10	42 ± 3	42 ± 2	42 ± 4	45 ± 5
IVSd (mm)	0.9 ± 0.1	1.0 ± 0.1	1.0 ± 0.1	1.0 ± 0.1	1.6 ± 0.2*	0.8 ± 0.2*	0.9 ± 0.1	0.9 ± 0.1	0.9 ± 0.1	1.0 ± 0.2	1.0 ± 0.1	1.0 ± 0.04
LVIDd (mm)	3.8 ± 0.2	3.7 ± 0.3	3.7 ± 0.2	3.4 ± 0.2	4.1 ± 0.5*	3.8 ± 0.3	3.6 ± 0.3	3.6 ± 0.1	3.3 ± 0.2	3.5 ± 0.4	4.4 ± 0.6*	3.6 ± 0.2
LVPWd (mm)	1.0 ± 0.1	1.0 ± 0.1	0.9 ± 0.1	0.9 ± 0.1	1.4 ± 0.2*	0.8 ± 0.2	0.9 ± 0.1	0.9 ± 0.1	1.0 ± 0.2	1.0 ± 0.1	1.1 ± 0.1	1.0 ± 0.1
IVSs (mm)	1.6 ± 0.2	1.5 ± 0.1	1.5 ± 0.2	1.9 ± 0.2	1.8 ± 0.2	1.2 ± 0.3*	1.7 ± 0.2	1.7 ± 0.2	1.5 ± 0.2	1.7 ± 0.3	1.7 ± 0.3	1.8 ± 0.3
LVIDs (mm)	2.1 ± 0.3	2.2 ± 0.3	2.0 ± 0.4	1.5 ± 0.3	3.2 ± 0.3*	2.6 ± 0.5*	1.8 ± 0.2	2.0 ± 0.1	2.0 ± 0.3	1.9 ± 0.5	2.7 ± 0.6*	1.6 ± 0.2
LVPWs (mm)	1.4 ± 0.2	1.4 ± 0.1	1.5 ± 0.3	1.5 ± 0.04	1.5 ± 0.3	1.1 ± 0.2*	1.2 ± 0.1	1.4 ± 0.2	1.3 ± 0.1	1.3 ± 0.1	1.4 ± 0.2	1.4 ± 0.2

Serial echo scans were acquired under isoflurane inhalational anaesthesia at baseline (Day 0), after 2-week treatment with ISO/vehicle (Day 14), and after a further 2 weeks following withdrawal of treatment (Day 28). *n* = 6/group. HR, heart rate; EF, ejection fraction; FS, fractional shortening; IVSd/s, interventricular septum diastole/systole; LVIDd/s, left ventricular internal dimension diastole/systole; LVPWd/s, left ventricular posterior wall diastole/systole.

\**P* < 0.05 vs. baseline (Day 0) within each genotype and treatment group.

susceptibility to both endogenous upstream inactivating kinases and exogenous pharmacological inhibitors,<sup>7,30</sup> thereby providing a more pragmatic strategy of interrogation and potential therapeutic targeting. Accordingly, while isoform-specific stress responses are likely, it is important to establish the combined effect of kinase manipulation *in vivo*. An example of this is seen with the protection against stress-induced interstitial fibrosis in dual isoform KI hearts in our study and in that previously reported using this model;<sup>22</sup> this contrasts with isolated overexpression of non-inhibitable GSK-3 $\alpha$ -isoforms, in which pressure overload significantly increases fibrosis.<sup>19</sup> Nevertheless, it is noteworthy in our results that interrogation of GSK-3 phosphorylation in response to acute ISO treatment in WT hearts (Figure 1B) revealed significant increases in N-terminal phosphorylation of the GSK-3 $\beta$ -isoform, compared with GSK-3 $\alpha$  and with baseline values. There were similar results at 14 days of ISO treatment (Figure 1C), suggesting dominance of GSK-3 $\beta$  inhibition over GSK-3 $\alpha$  during ISO stress signalling and, thus, by implication the predominant mechanism of protection in the double-KI mouse.

Consistent with early phenotype characterization,<sup>22</sup> we observed a small trend towards higher normalized HWs in male KI mice with increasing age (Figure 1). However, hypertrophy protocols undertaken in sex- and age-matched mice revealed no differences in baseline LV cavity dimensions or contractile performance between 8 and 10 weeks of age (Tables 1 and 2; see Supplementary material online, Table S2). Furthermore, extrapolation from two non-invasive modalities in control animal groups in our protocols suggests that this equivalence is maintained out to 12–14 weeks of age (Table 2; see Supplementary material online, Table S2).

KI hearts were protected against pharmacological-induced stress caused by subcutaneous administration of ISO at all levels of interrogation. Specifically, there was attenuation of hypertrophy, contractile dysfunction, interstitial fibrosis, apoptosis, and reactivation of pro-hypertrophic foetal gene programmes, all of which were significantly evident in WT hearts. Co-treatment with the pharmacological GSK-3 inhibitor BIO recovered susceptibility to myocardial hypertrophy and contractile dysfunction, but only in the presence of agonist. Interestingly, KI hearts did remodel in response to adrenergic stimulation with significant LV chamber dilatation (Figure 5 and Table 2; see Supplementary material online, Table S2). Since this was fully reversible and not associated with the pathological cellular and sub-cellular traits outlined previously, it is likely to reflect a 'positive remodelling' phenomenon, consistent with an adaptive physiological response. In keeping with this, there was a sustained sensitivity to acute adrenergic stimulation with ISO in isolated hearts (Figure 6B). This was in direct comparison to WT hearts which were desensitized after 2-week ISO, and in which the dose–response profile remained blunted after 2-week recovery without treatment. It is tempting to speculate that these reversible structural and functional changes in KI hearts mirror the positive remodelling characteristics of physiological hypertrophy and the athletic heart in humans.<sup>31,32</sup> Although no firm conclusions in this respect can be made from our experiments, it appears that targeting both GSK-3 isoforms is nevertheless safe over the experimental time frame examined.

The precise mechanisms involved in the protective effects of catalytically active GSK-3 remain unclear, although it is likely to involve regulation of gene and protein expression within the cardiomyocyte. Several downstream transcription and translational factors are directly regulated by GSK-3 activity.<sup>22</sup> Furthermore, nuclear

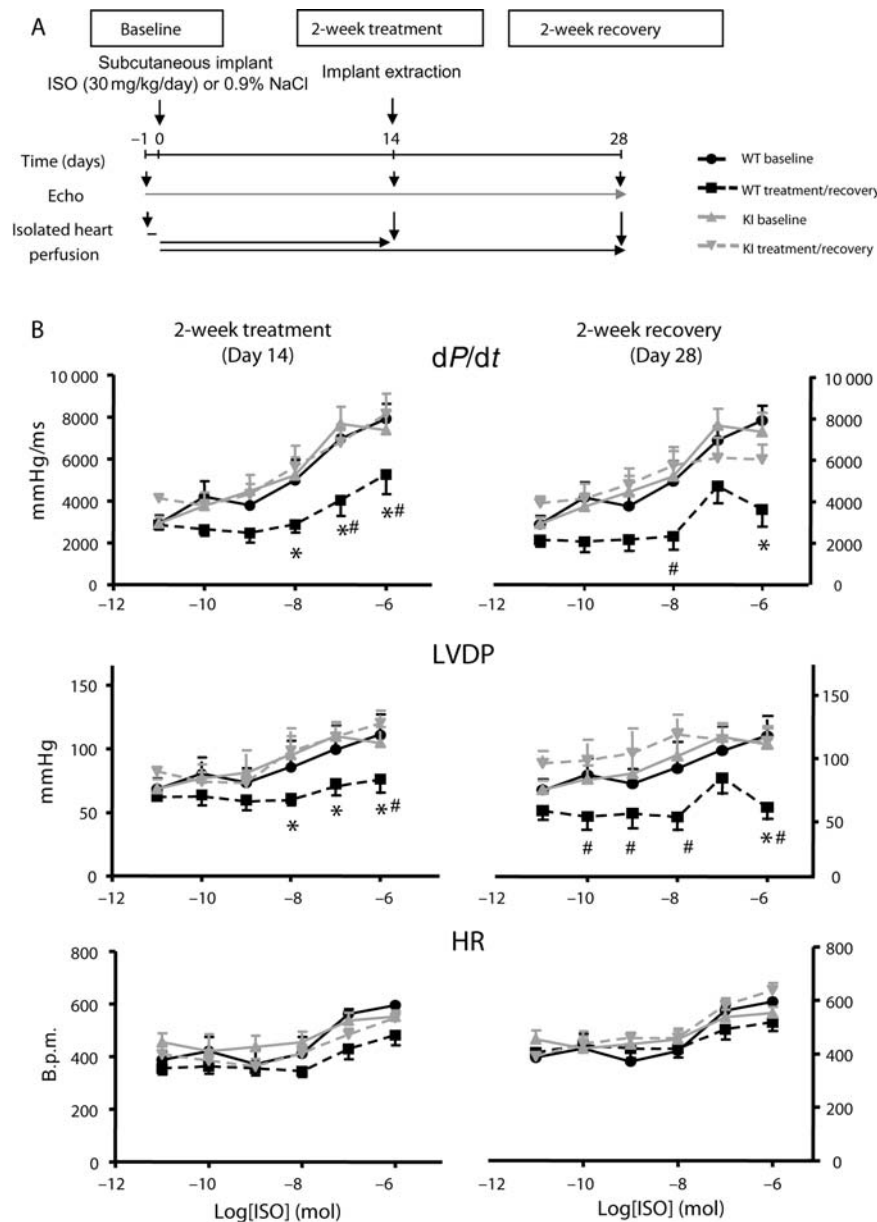


**Figure 6** Chronic ISO treatment and recovery. (A) Experimental protocol: mice were treated for 2 weeks with subcutaneous ISO or vehicle and recovered for 2 weeks after pump extraction. Serial echocardiography was performed at baseline, 14, and 28 days. Parallel experiments were undertaken in chronic ISO-treated animals and hearts explanted for Langendorff-perfusion to test acute adrenergic sensitivity. (B) Dose–response profiles to acute ISO exposure in isolated Langendorff-perfused hearts. Baseline response is compared with that at 2-week ISO treatment (left panel) and 2-week recovery (right panel), respectively. Absolute values are plotted. LVDP, left ventricular developed pressure, +dP/dt, systolic contractile performance; HR, heart rate;  $n = 6/\text{group}$ ,  $*P < 0.05$  vs. WT baseline,  $\#P < 0.05$  vs. KI treated/recovery groups.

content of GSK-3 increases with pharmacological and mechanical stress, although the extent and isoform preference of this remains unclear.<sup>22,33,34</sup> We undertook protein interrogation of related signalling partners in ISO-treated hearts, including cyclin-D1,  $\beta$ -catenin, p38, HDAC-2, and eif2B $\epsilon$ , but were unable to identify any consistent differences between genotypes (data not shown). It is also unclear whether protection in this model of constitutive GSK-3 activity would be afforded to other neurohormonal agonists *in vivo*, such as phenylephrine, endothelin-1, or angiotensin II. Ultimately, it is unlikely that a single kinase system integrates all pro-hypertrophic signalling pathways, emphasizing the need for biologically relevant

models in the characterization of relevant cardiomyocyte signalling and in determining the overall effects of single kinase interventions.

Although the genetic strategy employed in this study avoids the confounders of cardiac-specific transgene manipulation, other potential limitations have been highlighted in this model.<sup>22</sup> In particular, genetic manipulation of endogenous GSK-3 alleles may have non-selective consequences over and above those of merely preventing N-terminal phosphorylation and kinase inhibition. Furthermore, ubiquitous expression beyond the cardiomyocyte may exert important systemic or localized cardiovascular effects. It is

also acknowledged that the effects of pharmacological GSK-3 inhibition with BIO may reflect off-target phenomena.

In conclusion, our findings support a strategic and permissive role for GSK-3 signalling in maladaptive hypertrophic remodelling secondary to chronic adrenergic stimulation. Generic strategies to maintain GSK-3 $\alpha$ / $\beta$  active may prove a useful therapeutic target, but require further validation in other models of neurohormonal and pathophysiological stress.

## Supplementary material

Supplementary material is available at *Cardiovascular Research* online.

## Acknowledgements

We thank Professor Dario Alessi (Dundee, Scotland) for providing the GSK-3 mice.

**Conflict of interest:** none declared.

## Funding

This work was supported by a Wellcome Trust Project Grant (074653) and BHF Fellowships to I.G.W. (07/032) and J.E.C. (06/026).

## References

- Juhászova M, Zorov DB, Kim SH, Pepe S, Fu Q, Fishbein KW *et al.* Glycogen synthase kinase-3 $\beta$  mediates convergence of protection signaling to inhibit the mitochondrial permeability transition pore. *J Clin Invest* 2004;**113**:1535–1549.
- Tong H, Imahashi K, Steenbergen C, Murphy E. Phosphorylation of glycogen synthase kinase-3 $\beta$  during preconditioning through a phosphatidylinositol-3-kinase-dependent pathway is cardioprotective. *Circ Res* 2002;**90**:377–379.
- Antos CL, McKinsey TA, Frey N, Kutschke W, McAnally J, Shelton JM *et al.* Activated glycogen synthase-3  $\beta$  suppresses cardiac hypertrophy in vivo. *Proc Natl Acad Sci USA* 2002;**99**:907–912.
- Haq S, Choukroun G, Kang ZB, Ranu H, Matsui T, Rosenzweig A *et al.* Glycogen synthase kinase-3 $\beta$  is a negative regulator of cardiomyocyte hypertrophy. *J Cell Biol* 2000;**151**:117–130.
- Haq S, Choukroun G, Lim H, Tymitz KM, del Monte F, Gwathmey J *et al.* Differential activation of signal transduction pathways in human hearts with hypertrophy versus advanced heart failure. *Circulation* 2001;**103**:670–677.
- Hirota S, Zhai P, Tomita H, Galeotti J, Marquez JP, Gao S *et al.* Inhibition of glycogen synthase kinase 3 $\beta$  during heart failure is protective. *Circ Res* 2007;**101**:1164–1174.
- Meijer L, Flajolet M, Greengard P. Pharmacological inhibitors of glycogen synthase kinase 3. *Trends Pharmacol Sci* 2004;**25**:471–480.
- Allen DL, Harrison BC, Maass A, Bell ML, Byrnes WC, Leinwand LA. Cardiac and skeletal muscle adaptations to voluntary wheel running in the mouse. *J Appl Physiol* 2001;**90**:1900–1908.
- Eghbali M, Deva R, Alioua A, Minosyan TY, Ruan H, Wang Y *et al.* Molecular and functional signature of heart hypertrophy during pregnancy. *Circ Res* 2005;**96**:1208–1216.
- Izumo S, Lompre AM, Matsuoka R, Koren G, Schwartz K, Nadal-Ginard B *et al.* Myosin heavy chain messenger RNA and protein isoform transitions during cardiac hypertrophy. Interaction between hemodynamic and thyroid hormone-induced signals. *J Clin Invest* 1987;**79**:970–977.
- Michael A, Haq S, Chen X, Hsieh E, Cui L, Walters B *et al.* Glycogen synthase kinase-3  $\beta$  regulates growth, calcium homeostasis, and diastolic function in the heart. *J Biol Chem* 2004;**279**:21383–21393.
- Haq S, Michael A, Andreucci M, Bhattacharya K, Dotto P, Walters B *et al.* Stabilization of beta-catenin by a Wnt-independent mechanism regulates cardiomyocyte growth. *Proc Natl Acad Sci USA* 2003;**100**:4610–4615.
- Hardt SE, Tomita H, Katus HA, Sadoshima J. Phosphorylation of eukaryotic translation initiation factor 2B $\epsilon$  by glycogen synthase kinase-3 $\beta$  regulates beta-adrenergic cardiac myocyte hypertrophy. *Circ Res* 2004;**94**:926–935.
- Morisco C, Seta K, Hardt SE, Lee Y, Vatner SF, Sadoshima J. Glycogen synthase kinase 3 $\beta$  regulates GATA4 in cardiac myocytes. *J Biol Chem* 2001;**276**:28586–28597.
- Branaccio M, Guazzone S, Menini N, Sibona E, Hirsch E, De Andrea M *et al.* Melusin is a new muscle-specific interactor for beta(1) integrin cytoplasmic domain. *J Biol Chem* 1999;**274**:29282–29288.
- Morisco C, Zebrowski D, Condorelli G, Tschlis P, Vatner SF, Sadoshima J. The Akt-glycogen synthase kinase 3 $\beta$  pathway regulates transcription of atrial natriuretic factor induced by beta-adrenergic receptor stimulation in cardiac myocytes. *J Biol Chem* 2000;**275**:14466–14475.
- Luckey SW, Mansoori J, Fair K, Antos CL, Olson EN, Leinwand LA. Blocking cardiac growth in hypertrophic cardiomyopathy induces cardiac dysfunction and decreased survival only in males. *Am J Physiol Heart Circ Physiol* 2007;**292**:H838–H845.
- Sanbe A, Gulick J, Hanks MC, Liang Q, Osinska H, Robbins J. Reengineering inducible cardiac-specific transgenesis with an attenuated myosin heavy chain promoter. *Circ Res* 2003;**92**:609–616.
- Zhai P, Gao S, Holle E, Yu X, Yatani A, Wagner T *et al.* Glycogen synthase kinase-3 $\alpha$  reduces cardiac growth and pressure overload-induced cardiac hypertrophy by inhibition of extracellular signal-regulated kinases. *J Biol Chem* 2007;**282**:33181–33191.
- Cook SA, Clerk A, Sugden PH. Are transgenic mice the 'alkahest' to understanding myocardial hypertrophy and failure? *J Mol Cell Cardiol* 2008;**46**:118–129.
- McManus EJ, Sakamoto K, Armit LJ, Ronaldson L, Shapiro N, Marquez R *et al.* Role that phosphorylation of GSK3 plays in insulin and Wnt signalling defined by knockin analysis. *EMBO J* 2005;**24**:1571–1583.
- Matsuda T, Zhai P, Maejima Y, Hong C, Gao S, Tian B *et al.* Distinct roles of GSK-3 $\alpha$  and GSK-3 $\beta$  phosphorylation in the heart under pressure overload. *Proc Natl Acad Sci USA* 2008;**105**:20900–20905.
- Nishino Y, Webb IG, Davidson SM, Ahmed AI, Clark JE, Jacquet S *et al.* Glycogen synthase kinase-3 inactivation is not required for ischemic preconditioning or post-conditioning in the mouse. *Circ Res* 2008;**103**:307–314.
- Trivedi CM, Luo Y, Yin Z, Zhang M, Zhu W, Wang T *et al.* Hdac2 regulates the cardiac hypertrophic response by modulating Gsk3  $\beta$  activity. *Nat Med* 2007;**13**:324–331.
- Ducharme A, Frantz S, Aikawa M, Rabkin E, Lindsey M, Rohde LE *et al.* Targeted deletion of matrix metalloproteinase-9 attenuates left ventricular enlargement and collagen accumulation after experimental myocardial infarction. *J Clin Invest* 2000;**106**:55–62.
- Junqueira LC, Bignolas G, Brentani RR. Picrosirius staining plus polarization microscopy, a specific method for collagen detection in tissue sections. *Histochem J* 1979;**11**:447–455.
- Sugden PH, Fuller SJ, Weiss SC, Clerk A. Glycogen synthase kinase 3 (GSK3) in the heart: a point of integration in hypertrophic signalling and a therapeutic target? A critical analysis. *Br J Pharmacol* 2008;**153**:S137–S153.
- Schuyler GT, Yarbrough LR. Changes in myosin and creatine kinase mRNA levels with cardiac hypertrophy and hypothyroidism. *Basic Res Cardiol* 1990;**85**:481–494.
- Cook AR, Bardwell SC, Pretheshan S, Dighe K, Kaganayagam GS, Jabr RI *et al.* Paradoxical resistance to myocardial ischemia and age-related cardiomyopathy in NHE1 transgenic mice: a role for ER stress? *J Mol Cell Cardiol* 2009;**46**:225–233.
- Doble BW, Patel S, Wood GA, Kockeritz LK, Woodgett JR. Functional redundancy of GSK-3 $\alpha$  and GSK-3 $\beta$  in Wnt/beta-catenin signaling shown by using an allelic series of embryonic stem cell lines. *Dev Cell* 2007;**12**:957–971.
- Pluim BM, Zwinderman AH, van der LA, van der Wall EE. The athlete's heart. A meta-analysis of cardiac structure and function. *Circulation* 2000;**101**:336–344.
- De Castro S, Pelliccia A, Caselli S, Di Angelantonio E, Papetti F, Cavarretta E *et al.* Remodelling of the left ventricle in athlete's heart: a three dimensional echocardiographic and magnetic resonance imaging study. *Heart* 2006;**92**:975–976.
- Markou T, Cullingford TE, Giraldo A, Weiss SC, Alsafi A, Fuller SJ *et al.* Glycogen synthase kinases 3 $\alpha$  and 3 $\beta$  in cardiac myocytes: regulation and consequences of their inhibition. *Cell Signal* 2008;**20**:206–218.
- Menon B, Johnson JN, Ross RS, Singh M, Singh K. Glycogen synthase kinase-3 $\beta$  plays a pro-apoptotic role in beta-adrenergic receptor-stimulated apoptosis in adult rat ventricular myocytes: role of beta1 integrins. *J Mol Cell Cardiol* 2007;**42**:653–661.